

1 **Supplemental Methods, Data Figures, and Tables for Fortmann and Patton *et al.***
2 **“Circulating SARS-CoV-2+ Megakaryocytes Associate with Severe Viral Infection**
3 **in COVID-19”**

4
5 **Single-Cell RNA-Sequencing Analysis**

6 FASTQ files from 69 single-cell RNA-sequencing (scRNA-seq) samples were
7 downloaded from the European Nucleotide Archive or Gene Expression Omnibus. The
8 samples were derived from 4 separate studies (1-4), all of which used the droplet-based
9 10X Genomics platform. Two of the datasets used 3' RNA sequencing (1,3) and the other
10 two used 5' sequencing (2,4). Severity of infection for each patient was determined by the
11 original authors. Transcriptomic alignment, barcode demultiplexing, and gene count
12 quantification were done using Cell Ranger (version 3.1.0) with the force-cells option set
13 to 15,000. The reference transcriptome was GRCh38 and was downloaded from 10X
14 Genomics. All downstream analyses were done using Scanpy (version 1.6.0), a Python-
15 based suite of packages for scRNA-seq analysis. For quality control filtering, cells were
16 removed that contained >50,000 or <500 reads and >4,500 or <500 genes. Additionally,
17 mitochondrial and ribosomal gene percentage cutoffs of 20% and 50%, respectively, were
18 used to further eliminate low quality cells. Lastly, Scrublet (version 0.2.1) was used to
19 remove potential doublets. After quality control filtering, the 69 samples were
20 concatenated and 321,035 cells were recovered in total. Normalization was performed
21 using Scran (version 1.10.2), and Scanpy was then used to perform complete cell cycle
22 regression using the cell cycle genes identified by Tirosh *et al* (5). Scanpy was used to
23 select the top 2,000 highly variable genes, which were then used to calculate the top 20

24 principal components (PCs). Batch correction was performed using Harmony with the
25 Scanpy external application programming interface (**Figure S1**). Two categorical
26 covariates were used for Harmony integration, one designating individual samples and
27 the other designating one of four different datasets that each sample originated from.
28 Final dimensionality reduction was done using uniform manifold approximation and
29 projection (UMAP) with default settings. Clustering was performed using the Leiden
30 algorithm with a resolution of 0.8, and 14 clusters were identified. The assignment of
31 cluster identities was guided by the expression of lineage-specific marker genes (**Figure**
32 **S2**). One cluster composed of 12 total cells was identified as damaged red blood cells
33 and removed. The megakaryocyte (MK) cluster was identified by specific expression of
34 Integrin Subunit Beta 3 (ITGB3; CD61), Integrin Subunit Alpha 2b (ITGA2B; CD41), and
35 Platelet Glycoprotein Ib Alpha Chain (GP1BA; CD42b) and other MK/platelet marker
36 genes (**Figure S2**). Subclustering of the MKs revealed two populations, one of which was
37 contaminated with CD3+ T cells and was removed. The final dataset was composed of
38 317,574 total cells with 13 distinct clusters, including MKs (4,180 cells; **Figure S2**). Upon
39 publication, a GitHub repository will be posted containing all scRNA-seq data and
40 notebooks.

41 MK frequencies for each donor were calculated as the proportion of MKs compared
42 to all cells for a given sample. Median values for each group were used for Kruskal–Wallis
43 nonparametric one-way ANOVA with Dunn’s post-hoc multiple comparisons test
44 (GraphPad Prism, version 6.01). All groups were compared to uninfected controls.

45 Differential gene expression analysis was performed on normalized expression
46 data using MAST (version 1.8.2). MKs from severe COVID-19 patients were compared

47 to MKs from uninfected donors and the following covariates were included: number of
48 genes expressed per cell and the dataset that each cell originated from.

49 Mean MK-derived S100A8 and S100A9 gene expression was determined for each
50 donor. These individual donor values were then used to calculate the mean expression
51 of S100A8 and S100A9 per group. Statistical analyses of mean S100A8 and S100A9
52 gene expression per group were done using two-way ANOVA with Dunnett's post-hoc
53 multiple comparisons test (GraphPad Prism, version 6.01). All groups were compared to
54 uninfected controls.

55 **Flow Cytometry**

56 Cryopreserved cell suspensions were rapidly thawed in a 37°C water bath for 3
57 minutes and filtered through a 100µm strainer. 1mL of fresh FBS was added to each
58 sample followed by centrifugation at 1000xg for 5 minutes at 4°C. The samples were
59 resuspended in 1mL of flow cytometry staining buffer (FACS; phosphate-buffered saline
60 with 5% FBS, 2mM EDTA, and 0.1% sodium azide). 10µL of each sample was stained
61 with anti-CD61 (VI-PL2; AF647) and the concentration of CD61+ cells were determined
62 using flow cytometry. Ten million CD61+ cells were used to standardize each sample for
63 the final flow cytometry panel. Cell suspensions were surface stained at room
64 temperature for 30 minutes in 100µL of staining buffer (50µL of Brilliant Stain Buffer
65 (Becton Dickinson) and 50µL of FACS) with the following antibody cocktail: anti-CD61
66 (VI-PL2; BV605), anti-CD41 (HIP8; APC/Cy7), anti-CD45 (HI30; BV510), viability dye
67 (violet; Invitrogen), and Human TruStain FcX (BioLegend). Cells were fixed and
68 permeabilized with BD Cytotfix/Cytoperm (Becton Dickinson) for 30 minutes on ice. Cells
69 were intracellularly stained with anti-S100A8/A9 (27E10; Santa Cruz) and anti-spike

70 protein (P05DHuRb; Invitrogen) for 30 minutes on ice in 100 μ L of Perm/Wash Buffer
71 (Becton Dickinson). Finally, cells were incubated with 200 μ L RNase and propidium iodide
72 (PI/RNase Staining Buffer; Becton Dickinson) for 15 minutes at room temperature, per
73 the manufacturer's instruction. Each sample was resuspended in 300 μ L of FACS buffer
74 and analyzed with a three-laser FACSCelesta flow cytometer (Becton Dickinson). All 220
75 peripheral blood samples were analyzed in 6 batches during a 1 week period. FCS files
76 were analyzed using FlowJo (version 10.7). The gating scheme (**Figure S3**), fluorescence
77 minus one (FMO; **Figure S4**) controls, and isotype control stains for S100A8/A9 and spike
78 protein (**Figure S5**) are provided.

79 For quantification of specific proteins, the following antibodies were used: anti-
80 ACE2 (FAB933G[Novus]; AF488), anti-TMPRSS2 (H-4; AF488), anti-FURIN (B-6;
81 AF488), anti-p52/p100 (C-5; AF488), anti-p65 (F-6; AF488), anti-TLR2 (W15145C;
82 AF488), anti-TLR3 (TLR3.7; biotin), anti-TLR4 (HTA125; biotin), anti-ICAM1 (HA58;
83 APC/Fire750), anti-HLA-DR (G46-6; BV510), anti-CD62p (AK4; BV510), anti-activated
84 GPII/IIIa (PAC-1; FITC), anti-P2Y12 (S16001E; FITC), anti-PAR1 (ATAP2; AF488), anti-
85 CD66b (QA17A51; APC/Fire750), and anti-CD14 (M5E2; BV605). For PrimeFlow,
86 predesigned oligonucleotide probes against S100A8, S100A9, IFITM3, IFI27, SARS-
87 CoV-2, IL-6, IL-1 β , and TNF- α were purchased from Thermo Fisher and used according
88 to the manufacturer's instructions. For antibody stains, isotype controls were used for
89 calculating MFIs and percent positive quantifications. For PrimeFlow stains, the target
90 oligonucleotide was omitted for negative controls used in percent positive quantifications.
91 All other steps, including amplifications and fluorophore staining, for PrimeFlow were
92 identical across negative controls and experimental samples.

93 **FACS Sorting and Imaging Flow Cytometry**

94 Residual samples that were stained for the 218 patient cohort were pooled
95 together and used for fluorescence activated cell sorting (FACS) and imaging flow
96 cytometry experiments. The three megakaryocyte subpopulations, S100A8/A9- virus-,
97 S100A8/A9+ virus-, and S100A8/A9+ virus+, were FACS sorted using a FACSAria II
98 (Becton Dickinson). The cells were then pelleted with centrifugation and 3,000 cells per
99 subpopulation were resuspended in 20 μ L of FACS buffer (phosphate buffered saline with
100 5% FBS, 2mM EDTA, and 0.1% sodium azide). The samples were run on an Amnis
101 ImageStream^X Mk II System and were analyzed using the IDEAS software (version 6.2).
102 Mouse splenocytes were used for compensation controls. Identical image display
103 mapping values (X range: min & max and midpoint: x & y) for each specific channel were
104 uniformly applied to the three megakaryocyte samples before the final images were
105 exported.

106 **Immunofluorescence Staining of Lung and Brain Tissues**

107 Lungs from a deceased COVID-19 donor with acute respiratory distress syndrome
108 (ARDS) were inflated isobarically with 10% formalin. Brains from 8 deceased COVID-19
109 donors were fixed in 10% formalin and dissected to obtain sections from the frontal cortex,
110 pons, and medulla. Both lung and brain specimens were processed using standard tissue
111 processing techniques (dehydration, clearing, and infiltration), embedded in paraffin
112 blocks, sequential 5 μ m tissue sections were cut, and transferred on to positively charged
113 glass slides. The slides were incubated for 2 hours at 60°C. Deparaffinization and
114 rehydration of the slides was performed with three sequential 5 minute incubations in
115 xylene, two sequential 5 minute incubations in 100% ethanol, two sequential 5 minute

116 incubations in 95% ethanol, and washed in distilled water in three sequential 5 minute
117 incubations with gentle agitation. Citrate buffer (Vector Laboratories) prewarmed to 70°C
118 was used for antigen retrieval and was incubated in a heated steamer for 20 minutes,
119 followed by three washes in distilled water with gentle agitation. Sections were incubated
120 with 1X phosphate buffered saline (PBS) for 10 minutes and were then blocked with
121 Trident Universal Protein Blocking Reagent (GeneTex; GTX30963) and Human TruStain
122 FcX (Biolegend) at room temperature for 45 minutes. Sections were then stained
123 overnight in Trident Universal Protein Blocking Reagent at 4°C with the following
124 conjugated antibodies: anti-CD61 (FITC; VI-PL2), anti-S100A8/A9 (PE; 27E10; Santa
125 Cruz), and anti-spike protein (AF647; P05DHuRb; Invitrogen). Sections were washed with
126 gentle agitation at room temperature using excess 1X Tris-Buffered Saline with 0.01%
127 Triton x-100. Nuclear staining was done using Hoechst. Lastly, the sections were treated
128 with TrueVIEW Autofluorescence Quencher (Vector Laboratories) following the
129 manufacturer's instructions and were mounted using ProLong Gold Antifade Mountant
130 (Invitrogen). Images were collected using a Zeiss Axio Imager Z2 upright microscope.
131 Negative control stains were done using a mouse isotype antibody conjugated to AF488
132 (Invitrogen).

133 **Primary Human Megakaryocyte Experiments**

134 Primary human megakaryocytes were produced from CD34+ cord blood using the
135 Stem Cell Technologies StemSpan™ Megakaryocyte Expansion Supplement, according
136 to the manufacturer's instructions. Briefly, highly enriched CD34+ cord blood was
137 purchased from Stem Cell Technologies. 6 separate cultures were initiated in
138 StemSpan™ SFEM II media with Megakaryocyte Expansion Supplement and were

139 differentiated for 1 month. Cultures were assessed for morphologic and surface
140 expression changes (CD41, CD61, CD42b) consistent with MK phenotype. At 1 month,
141 MKs were enriched using anti-CD61 beads (Miltenyi Biotec), with an average purity of
142 ~95% MKs. The cultures were then inoculated with SARS-CoV-2 (MOI=2) for 24h. The
143 inoculant was removed, and the cells were then chemically induced to produce platelets
144 using phorbol ester myristate acetate (PMA; 10ng/mL) for 96h. Platelets were identified
145 with flow cytometry, using a similar gating scheme to that described earlier (**Figure S7**),
146 and were assessed for expression of spike protein. For immunofluorescence, infected
147 primary human megakaryocytes and non-infected controls, were moved to glass slides
148 coated with Attachment Factor (Cell Systems) following removal of inoculant and were
149 subsequently cultured for 96h in the presence of 10ng/mL PMA. Cells were stained with
150 anti-CD61 (FITC), anti-spike protein (AF647), anti-acetylated tubulin (6-11B-1;
151 unconjugated), and DAPI. Acetylated tubulin was counterstained with an anti-mouse
152 secondary antibody conjugated to AF594, prior to staining with the conjugated antibodies.

153 **Statistics**

154 *Flow Cytometry*

155 Student's t-test was used when two groups were being compared. ANOVA was
156 used when more than two groups were being compared. GraphPad Prism (version 6.01)
157 was used for statistical analyses.

158 *Clinical Correlations and Outcomes*

159 Statistically significant correlations between continuous patient variables,
160 cumulative 60-day outcomes, and patient MK proportions were determined using

161 Spearman correlation analysis. For analyses comparing MK frequencies with COVID-19
162 severity, statistical significance was assessed using the Dunn and Durbin-Conover tests
163 with median values from each nonparametric distribution and adjusted for multiple
164 comparisons with the Bonferroni method. Multivariate logistic regression models were
165 used to determine the associations between MK frequencies and the likelihood of 30-day
166 clinical outcomes. Adjusted odds ratios represent the predicted change in likelihood for a
167 20% increase in MK subpopulation frequencies (see **Tables S2-S4**, for model details).
168 Statistical significance for the multivariate logistic regression was assessed with the Wald
169 test and bootstrapped 95% confidence intervals were generated using 1000 iterations. All
170 figures, tables, modeling, and correlation analyses were performed and generated using
171 R version 4.2. Corresponding code will be openly available online at time of publication.

172

173

174

175

176

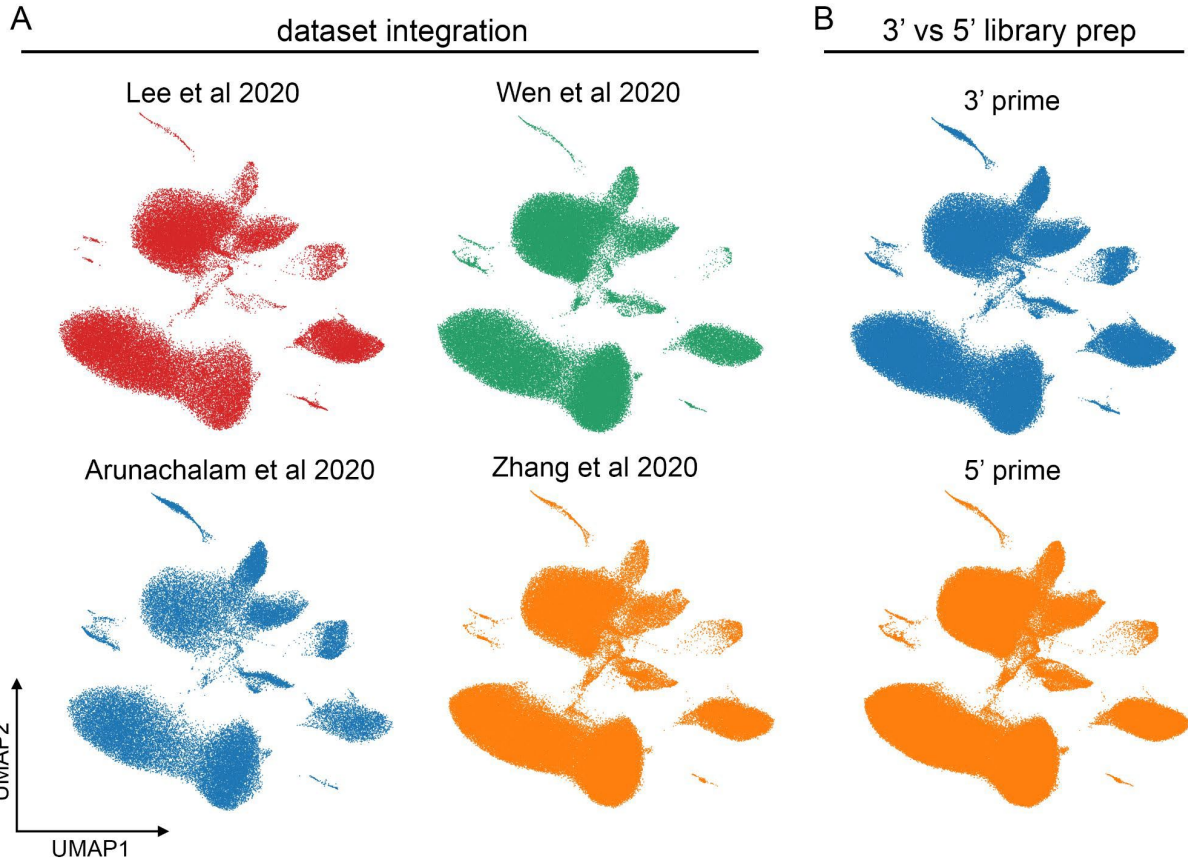
177

178

179

180

181



182

183 **Supplemental Figure 1. Single-cell RNA-sequencing batch correction.** Harmony
 184 integration successfully resolves batch effect by **(A)** dataset and **(B)** 3'/5' library
 185 preparation.

186

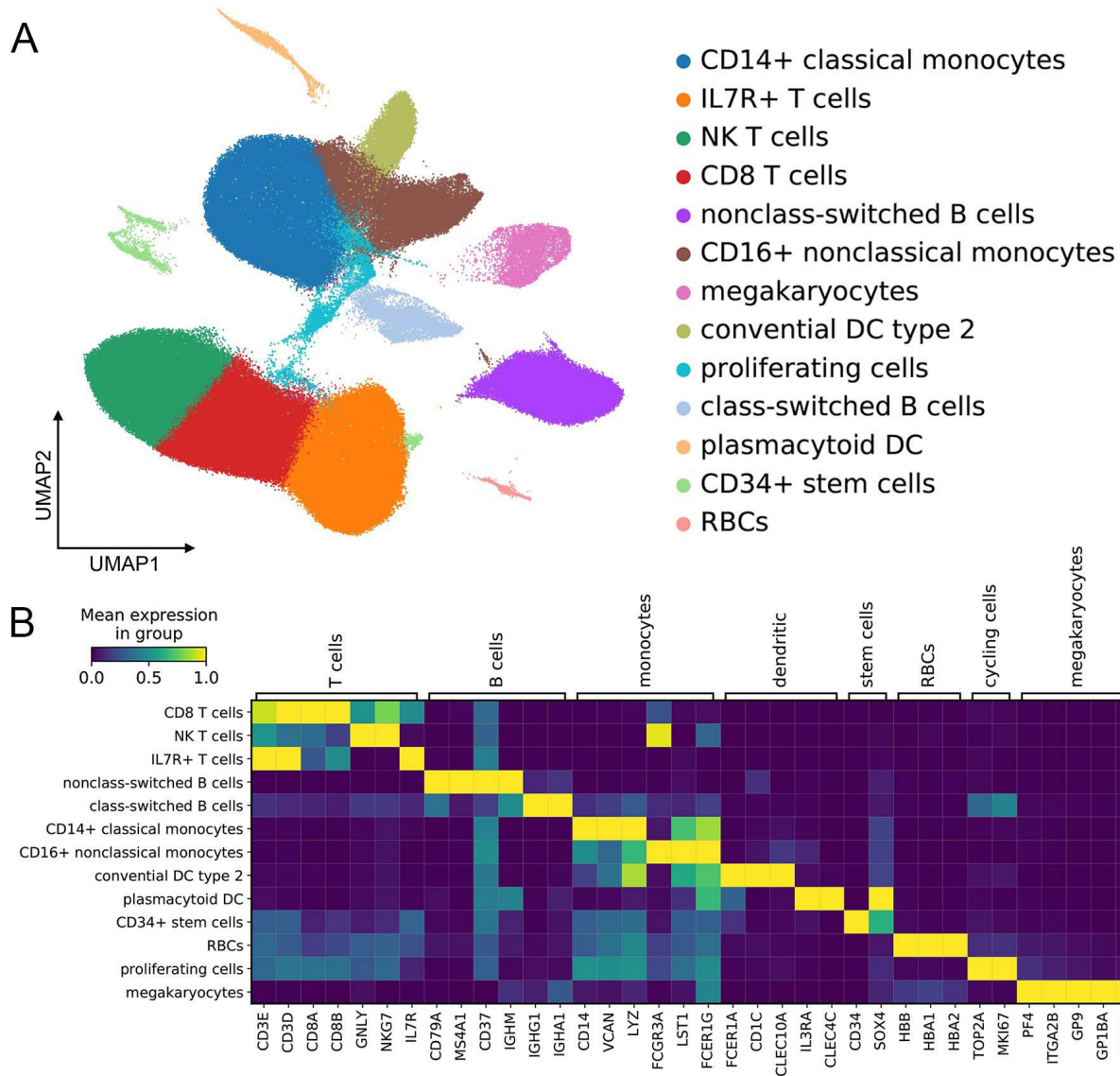
187

188

189

190

191



192

193 **Supplemental Figure 2. Single-cell RNA-sequencing of peripheral blood in COVID-**

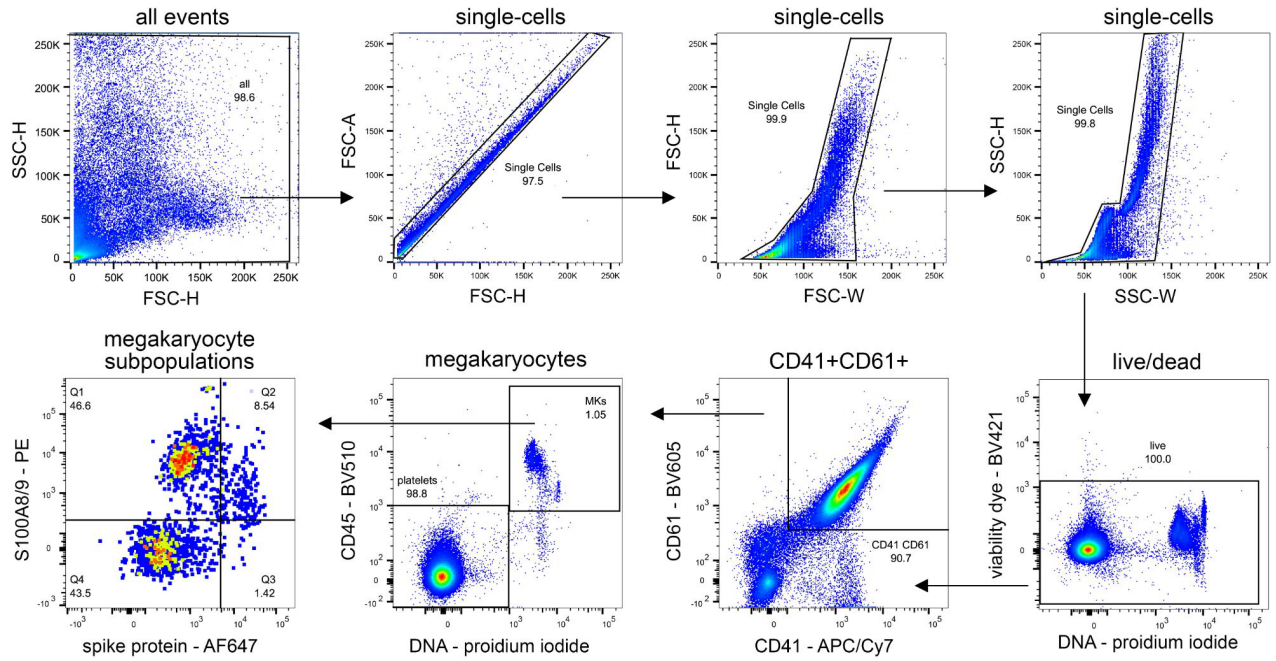
194 **19. (A)** UMAP projection of 317,574 cells showing 13 distinct cell populations. **(B)** Marker

195 gene expression for each cluster.

196

197

198



199

200 **Supplemental Figure 3. Flow cytometry gating scheme for circulating**
 201 **megakaryocytes.**

202

203

204

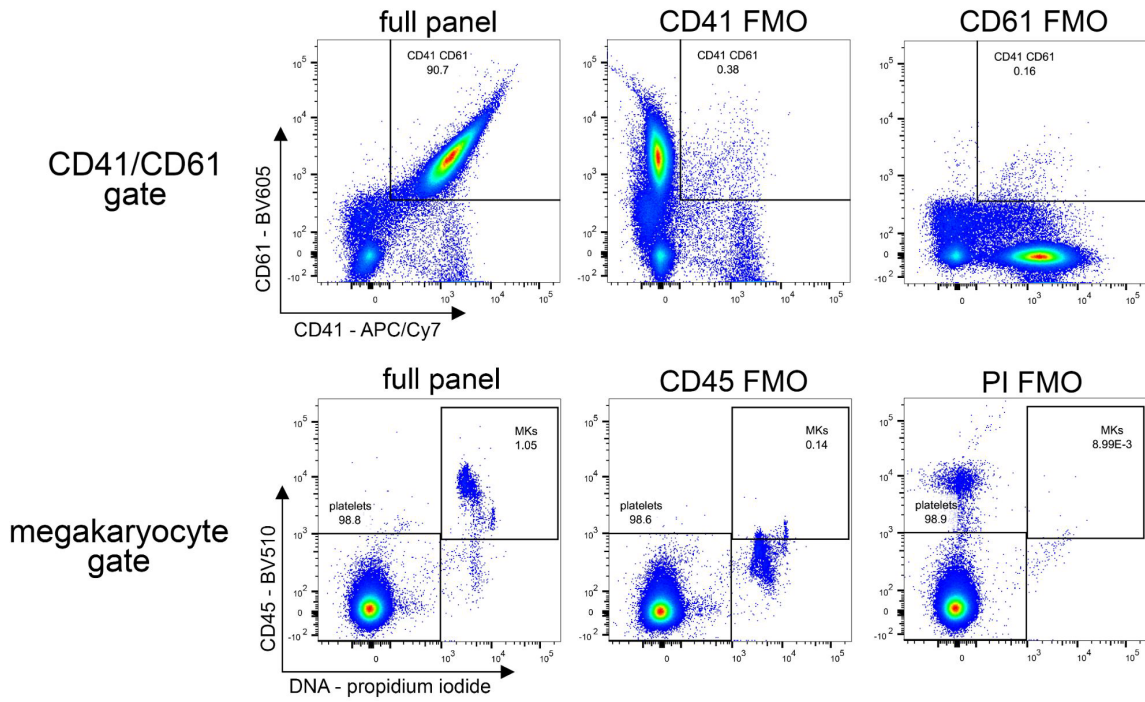
205

206

207

208

209



210

211 **Supplemental Figure 4. Fluorescence minus one (FMO) flow cytometry controls.**

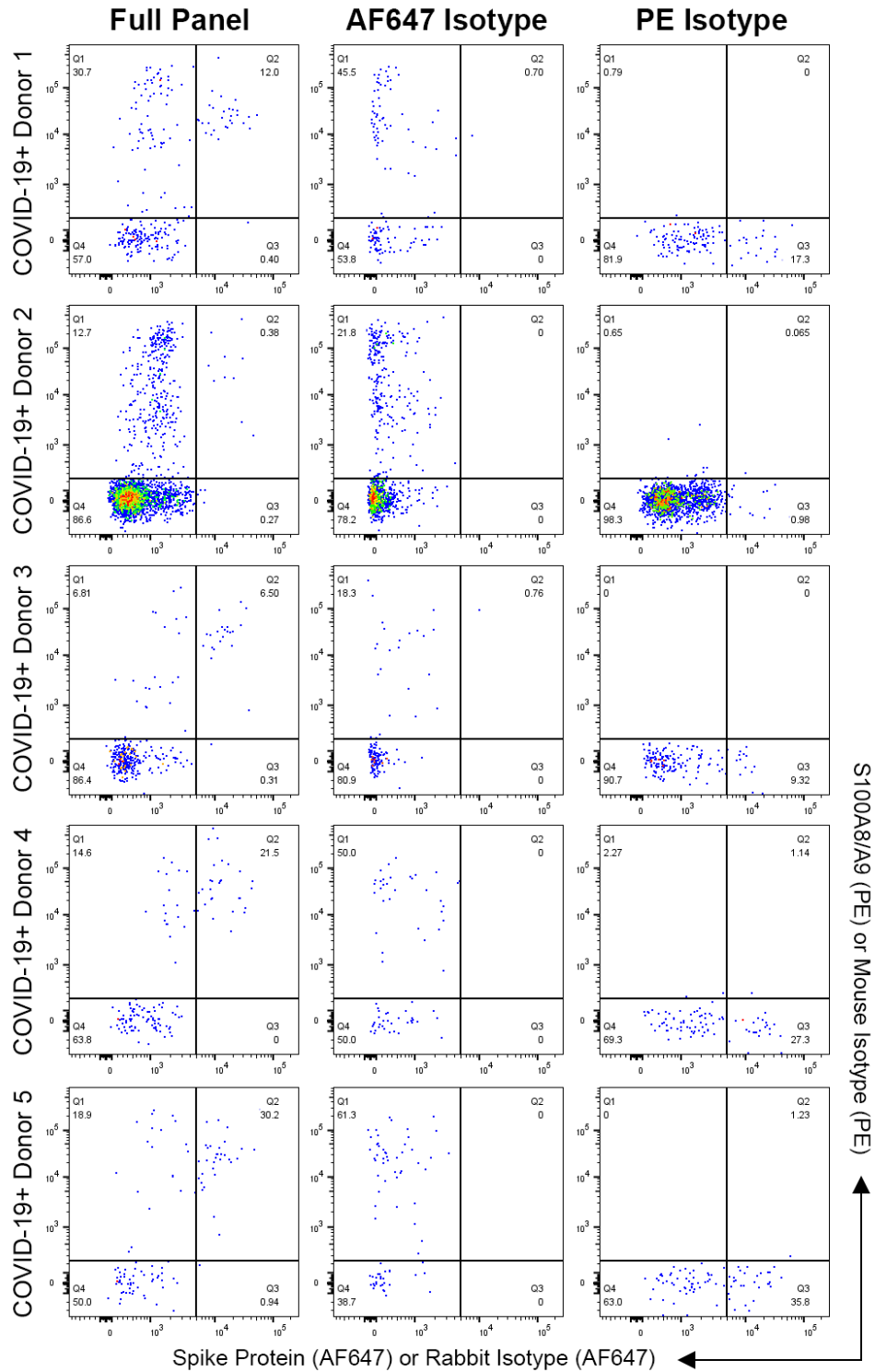
212

213

214

215

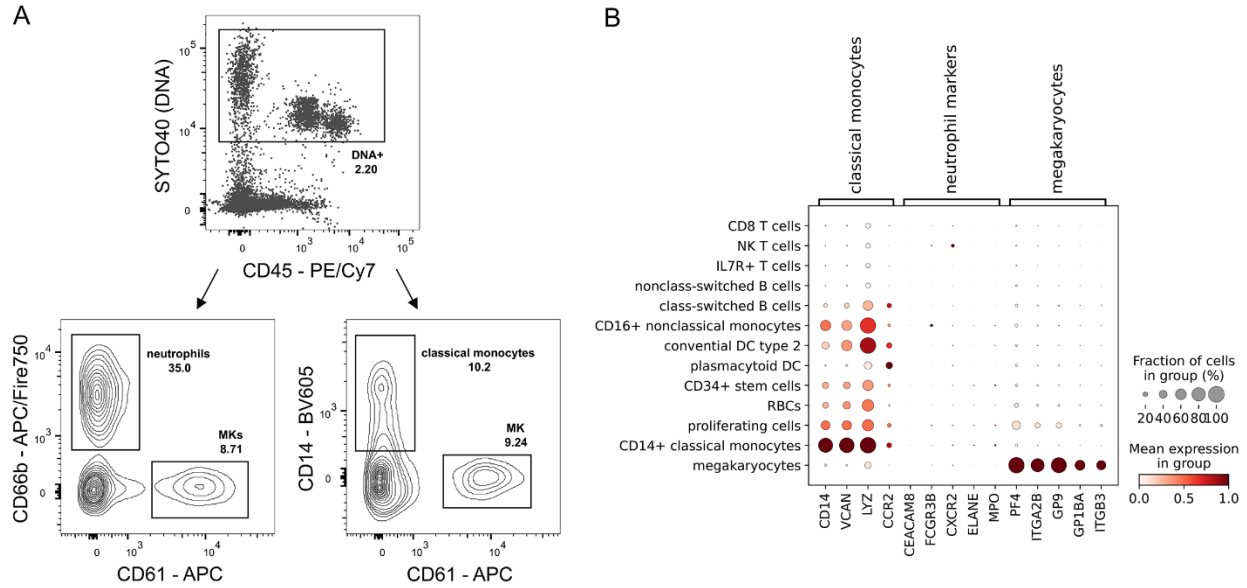
216



217

218 **Supplemental Figure 5. Isotype control stains for S100A8/A9 and spike protein from**

219 **five COVID-19+ donors.**



220

221 **Supplemental Figure 6. Circulating megakaryocytes lack expression of neutrophil**

222 **and classical monocyte markers. (A)** Representative flow cytometry staining for

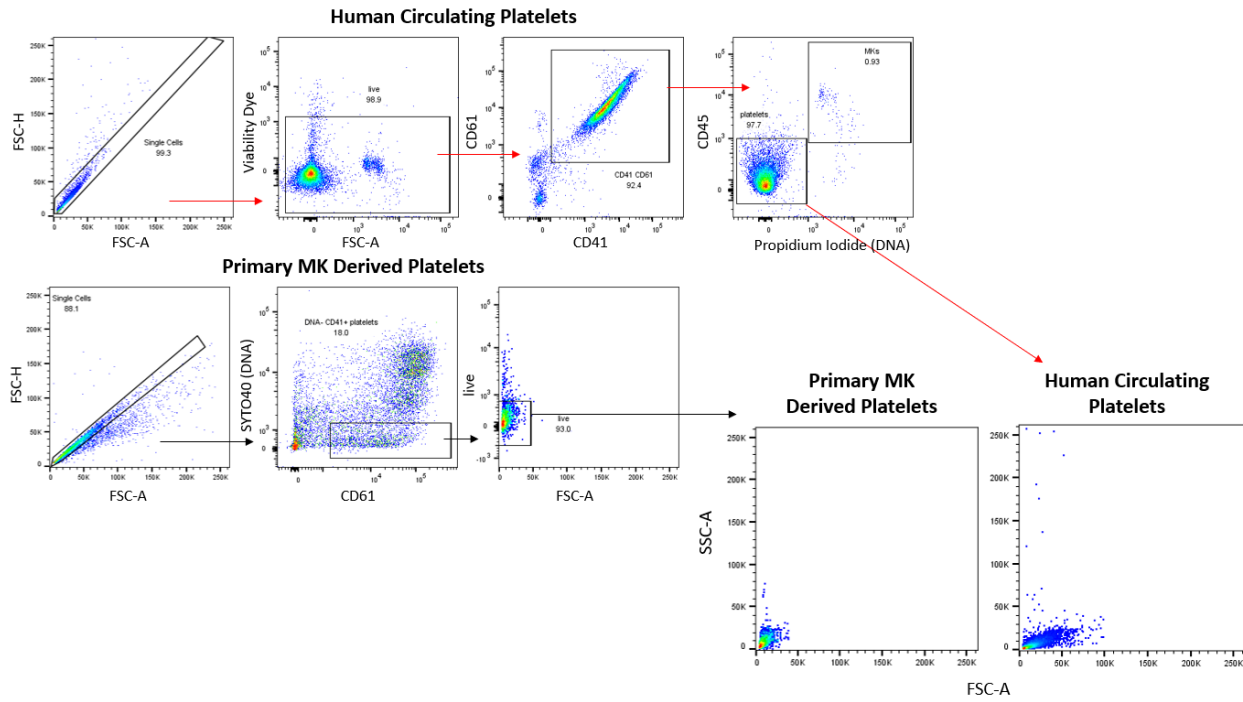
223 neutrophil (CD66b) and classical monocyte (CD14) markers versus CD61 in DNA+ live

224 cells. **(B)** Single-cell RNA-sequencing (scRNA-seq) data showing gene expression per

225 cluster for markers associated with classical monocytes, neutrophils, and

226 megakaryocytes. Note that neutrophils are not present in this scRNA-seq dataset,

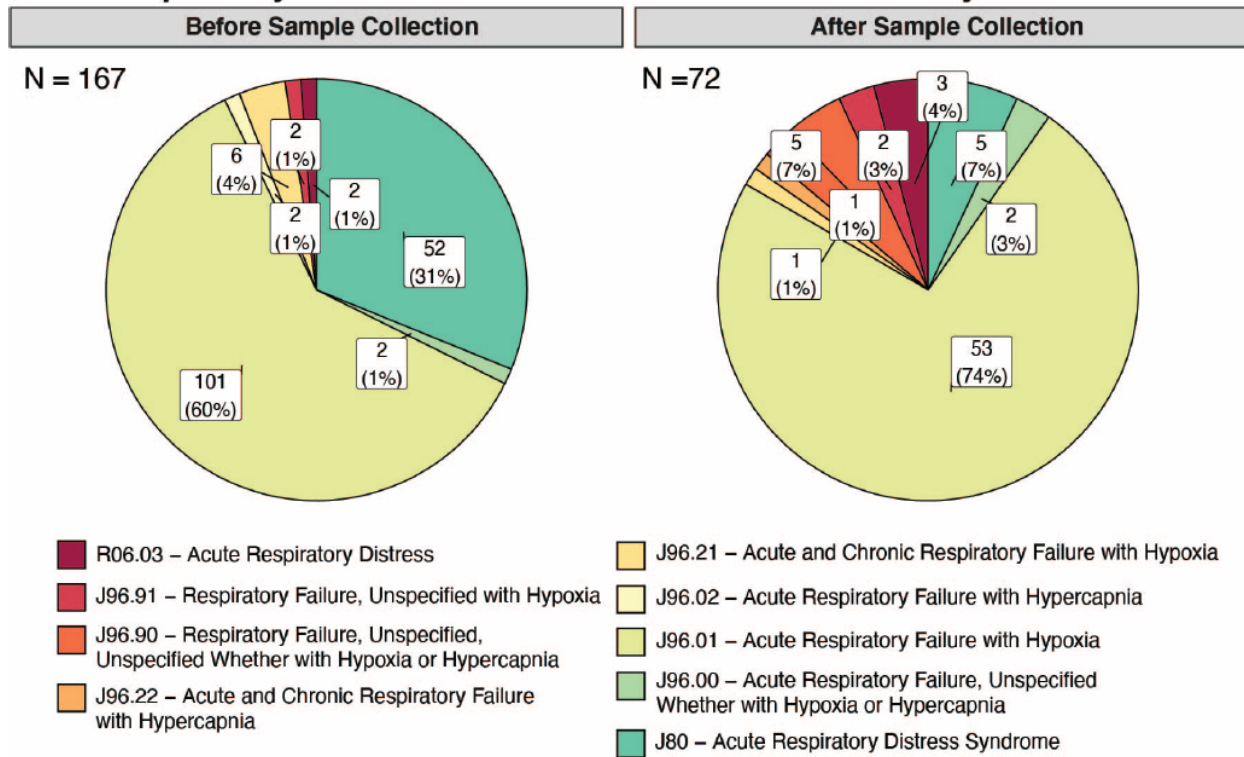
227 consistent with original publications of the data (1-4).



228

229 **Supplemental Figure 7. Flow cytometry gating scheme for primary megakaryocyte-**
 230 **derived platelets and comparison with human circulating platelets.**

Respiratory Failure Clinical Outcome Distributions by ICD10 Code



231

232 **Supplemental Figure 8. Distribution of Respiratory Failure Clinical Outcomes. ICD-**

233 10 code derived outcomes were assessed at two time-points: 1) the first respiratory failure

234 outcome found post COVID-19+ admission and prior to blood sample collection, 2) the

235 first respiratory failure outcome found post COVID-19+ admission, within 60-days after

236 blood sample collection. Total outcome count for each time-point (N) are noted in the

237 upper left hand corner of each pie-chart.

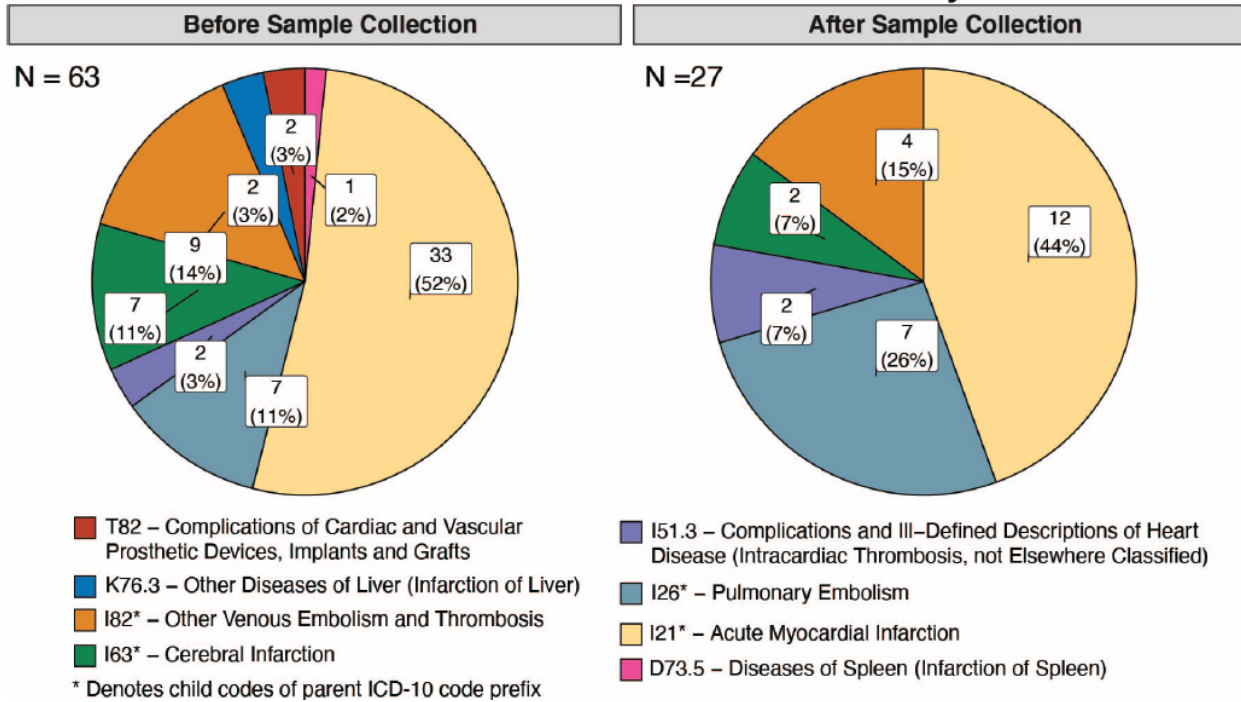
238

239

240

241

Thrombotic Event Clinical Outcome Distributions by ICD10 Code



242

243 **Supplemental Figure 9. Distribution of Thrombotic Event Clinical Outcomes. ICD-**

244 10 code derived outcomes were assessed at two time-points: 1) the first thrombotic event

245 outcome found post COVID-19+ admission and prior to blood sample collection, 2) the

246 first thrombotic event outcome found post COVID-19+ admission, within 60-days after

247 blood sample collection. Total outcome count for each time-point (N) are noted in the

248 upper left hand corner of each pie-chart.

249

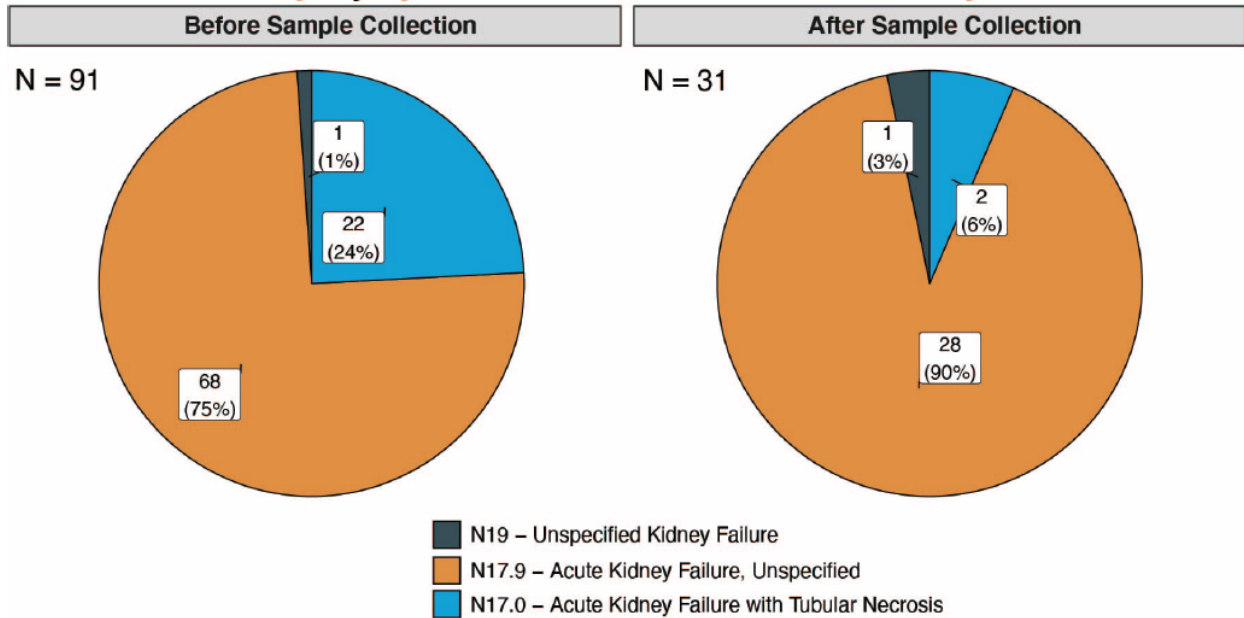
250

251

252

253

Acute Kidney Injury Clinical Outcome Distributions by ICD10 Code



254

255 **Supplemental Figure 10. Distribution of Acute Kidney Injury Clinical Outcomes.**

256 ICD-10 code derived outcomes were assessed at two time-points: 1) the first acute kidney
257 injury outcome found post COVID-19+ admission and prior to blood sample collection, 2)
258 the first acute kidney injury outcome found post COVID-19+ admission, within 60-days
259 after blood sample collection. Total outcome count for each time-point (N) are noted in
260 the upper left hand corner of each pie-chart.

261

262

263

264

265

266

Clinical Outcomes	ICD10 Codes
Thrombotic Events	I21.A1, I21.4, I63.9, I51.3, I24.0, I26.99, I82.409, I26.94, I82.401, I82.629, I82.413, I82.412, I21.01, I21.19, I22.2, I82.90, I82.411, I26.93, I82.403, I82.432, I82.811, I63.511, I21.3, I82.442, I82.452, I82.C11, I82.A13, I82.B12, I82.612, T82.868A, G45.9, I63.40, I82.621, I82.441, I82.431, I82.451, I82.C12, I82.210, D73.5, I81, I82.402, K76.3, N28.0, I63.431, I63.113, I21.9, I63.541, I21.11, I82.B11, I82.813, I82.A11, I82.611
Acute Kidney Injury	N17.9, N19, N17.0
Respiratory Failure	J96.01, J80, J96.21, J96.91, J96.90, J96.00, R06.03, J96.02, J96.92, J96.22

267

268

Table S1. ICD10 Billing Codes Used for Clinical Outcomes.

269

270

271

272

273

274

275

276

277

Model Variable	30-day Outcome	
	Adjusted OR (95% CI) ²	p-value ³
Respiratory Failure		
Age (per 1 year)	1.03 (1.00, 1.08)	0.068
Body Mass Index (per 1 point)	1.00 (0.94, 1.05)	0.96
Charlson Comorbidity Score (per 1 point)	1.19 (0.98, 1.48)	0.067
S100A8/A9+ Spike+ Megakaryocyte Proportion (per 20% increase)	2.42 (1.55, 4.36)	<0.001
ICU Admission		
Age (per 1 year)	1.01 (0.97, 1.06)	0.55
Body Mass Index (per 1 point)	1.01 (0.95, 1.05)	0.74
Charlson Comorbidity Score (per 1 point)	1.32 (1.07, 1.69)	0.012
S100A8/A9+ Spike+ Megakaryocyte Proportion (per 20% increase)	2.05 (1.05, 3.64)	0.011
Acute Kidney Injury		
Age (per 1 year)	1.01 (0.97, 1.05)	0.73
Body Mass Index (per 1 point)	1.01 (0.96, 1.04)	0.83
Charlson Comorbidity Score (per 1 point)	1.21 (1.02, 1.46)	0.039
S100A8/A9+ Spike+ Megakaryocyte Proportion (per 20% increase)	1.82 (1.12, 2.96)	0.010
Thrombotic Events		
Age (per 1 year)	1.00 (0.95, 1.05)	0.93
Body Mass Index (per 1 point)	0.99 (0.94, 1.03)	0.70
Charlson Comorbidity Score (per 1 point)	1.04 (0.85, 1.26)	0.70
S100A8/A9+ Spike+ Megakaryocyte Proportion (per 20% increase)	1.91 (1.13, 3.15)	0.012
Mechanical Ventilation		
Age (per 1 year)	0.99 (0.95, 1.04)	0.77
Body Mass Index (per 1 point)	0.97 (0.92, 1.03)	0.47
Charlson Comorbidity Score (per 1 point)	1.02 (0.81, 1.26)	0.82
S100A8/A9+ Spike+ Megakaryocyte Proportion (per 20% increase)	2.75 (1.48, 5.56)	<0.001
Mortality		
Age (per 1 year)	1.02 (0.99, 1.05)	0.16
Body Mass Index (per 1 point)	0.99 (0.96, 1.02)	0.56
Charlson Comorbidity Score (per 1 point)	0.96 (0.83, 1.12)	0.59
S100A8/A9+ Spike+ Megakaryocyte Proportion (per 20% increase)	1.71 (1.18, 2.51)	0.005

¹ OR = Odds Ratio

² Bootstrapped 95% Confidence Intervals (n=1,000)

³ Wald Test

278

279 **Table S2: Logistic Regression Models for 20% Increase in S100A8/A9+ Virus+**

280

Megakaryocyte Proportion for 30-day Adverse Events.

Model Variable	30-day Outcome	
	Adjusted OR (95% CI) ²	p-value ³
Respiratory Failure		
Age (per 1 year)	1.04 (1.01, 1.09)	0.027
Body Mass Index (per 1 point)	0.99 (0.94, 1.03)	0.78
Charlson Comorbidity Score (per 1 point)	1.19 (0.99, 1.43)	0.058
S100A8/A9+ Spike- Megakaryocyte Proportion (per 20% increase)	0.80 (0.46, 1.34)	0.37
ICU Admission		
Age (per 1 year)	1.02 (0.98, 1.06)	0.42
Body Mass Index (per 1 point)	1.00 (0.95, 1.04)	0.94
Charlson Comorbidity Score (per 1 point)	1.31 (1.06, 1.67)	0.011
S100A8/A9+ Spike- Megakaryocyte Proportion (per 20% increase)	0.99 (0.48, 2.29)	>0.99
Acute Kidney Injury		
Age (per 1 year)	1.01 (0.98, 1.05)	0.52
Body Mass Index (per 1 point)	1.00 (0.95, 1.04)	0.92
Charlson Comorbidity Score (per 1 point)	1.23 (1.00, 1.48)	0.034
S100A8/A9+ Spike- Megakaryocyte Proportion (per 20% increase)	0.99 (0.60, 1.74)	0.94
Thrombotic Events		
Age (per 1 year)	1.01 (0.97, 1.06)	0.78
Body Mass Index (per 1 point)	0.99 (0.93, 1.03)	0.60
Charlson Comorbidity Score (per 1 point)	1.06 (0.86, 1.26)	0.59
S100A8/A9+ Spike- Megakaryocyte Proportion (per 20% increase)	0.79 (0.44, 1.44)	0.45
Mechanical Ventilation		
Age (per 1 year)	1.01 (0.97, 1.05)	0.66
Body Mass Index (per 1 point)	0.97 (0.92, 1.01)	0.37
Charlson Comorbidity Score (per 1 point)	1.04 (0.79, 1.30)	0.70
S100A8/A9+ Spike- Megakaryocyte Proportion (per 20% increase)	1.06 (0.49, 2.43)	0.89
Mortality		
Age (per 1 year)	1.02 (1.00, 1.05)	0.056
Body Mass Index (per 1 point)	0.98 (0.95, 1.02)	0.42
Charlson Comorbidity Score (per 1 point)	0.96 (0.82, 1.10)	0.61
S100A8/A9+ Spike- Megakaryocyte Proportion (per 20% increase)	1.16 (0.76, 1.79)	0.44

¹ OR = Odds Ratio

² Bootstrapped 95% Confidence Intervals (n=1,000)

³ Wald Test

281

282 **Table S3: Logistic Regression Models for 20% Increase in S100A8/A9+ Virus-**

283 **Megakaryocyte Proportion for 30-day Adverse Events.**

Model Variable	30-day Outcome	
	Adjusted OR (95% CI) ²	p-value ³
Respiratory Failure		
Age (per 1 year)	1.04 (1.00, 1.09)	0.034
Body Mass Index (per 1 point)	1.00 (0.94, 1.04)	0.81
Charlson Comorbidity Score (per 1 point)	1.17 (0.97, 1.43)	0.10
S100A8/A9- Spike- Megakaryocyte Proportion (per 20% increase)	0.48 (0.19, 0.80)	0.006
ICU Admission		
Age (per 1 year)	1.02 (0.98, 1.06)	0.5
Body Mass Index (per 1 point)	1.00 (0.95, 1.05)	0.8
Charlson Comorbidity Score (per 1 point)	1.32 (1.08, 1.74)	0.008
S100A8/A9- Spike- Megakaryocyte Proportion (per 20% increase)	0.43 (0.19, 0.76)	0.002
Acute Kidney Injury		
Age (per 1 year)	1.01 (0.98, 1.05)	0.6
Body Mass Index (per 1 point)	1.00 (0.96, 1.04)	>0.9
Charlson Comorbidity Score (per 1 point)	1.20 (0.99, 1.46)	0.054
S100A8/A9- Spike- Megakaryocyte Proportion (per 20% increase)	0.56 (0.29, 0.89)	0.010
Thrombotic Events		
Age (per 1 year)	1.00 (0.96, 1.05)	0.9
Body Mass Index (per 1 point)	0.99 (0.93, 1.03)	0.5
Charlson Comorbidity Score (per 1 point)	1.03 (0.84, 1.25)	0.8
S100A8/A9- Spike- Megakaryocyte Proportion (per 20% increase)	0.63 (0.32, 1.02)	0.064
Mechanical Ventilation		
Age (per 1 year)	1.00 (0.96, 1.04)	0.9
Body Mass Index (per 1 point)	0.98 (0.92, 1.03)	0.4
Charlson Comorbidity Score (per 1 point)	0.99 (0.77, 1.27)	>0.9
S100A8/A9- Spike- Megakaryocyte Proportion (per 20% increase)	0.23 (0.08, 0.45)	<0.001
Mortality		
Age (per 1 year)	1.02 (1.00, 1.05)	0.10
Body Mass Index (per 1 point)	0.99 (0.96, 1.02)	0.4
Charlson Comorbidity Score (per 1 point)	0.94 (0.81, 1.10)	0.5
S100A8/A9- Spike- Megakaryocyte Proportion (per 20% increase)	0.57 (0.37, 0.81)	0.004

¹ OR = Odds Ratio

² Bootstrapped 95% Confidence Intervals (n=1,000)

³ Wald Test

284

285 **Table S4: Logistic Regression Models for 20% Increase in S100A8/A9- Virus-**

286 **Megakaryocyte Proportion for 30-day Adverse Events.**

Characteristic	Overall N = 218 ¹	Diabetic History N = 119 ¹	No Diabetic History N = 99 ¹	p-value
Age (years)	62 (52-70)	62 (52-69)	62 (54-72)	0.8 ²
Sex				0.4 ³
Female	92 (42%)	47 (39%)	45 (45%)	
Male	126 (58%)	72 (61%)	54 (55%)	
Charlson Comorbidity Score	3 (1-4)	3 (2-5)	2 (0-3)	<0.001 ²
Body Mass Index	32 (28-37)	33 (28-38)	31 (27-35)	0.15 ²
Calprotectin+ Spike+ Megakaryocyte Grouping				0.2 ³
Low (<12.8%)	72 (33%)	42 (35%)	30 (31%)	
Medium (12.8-27.7%)	72 (33%)	43 (36%)	29 (30%)	
High (>27.7%)	73 (34%)	34 (29%)	39 (40%)	
Inpatient Outcomes (within 30-days)				
Mechanical Ventilation	20 (9.2%)	10 (8.4%)	10 (10%)	0.6 ³
Respiratory Failure	69 (32%)	37 (31%)	32 (33%)	0.8 ³
Acute Kidney Injury	30 (14%)	19 (16%)	11 (11%)	0.3 ³
Thrombotic Event	25 (12%)	10 (8.4%)	15 (15%)	0.11 ³
Mortality	35 (16%)	23 (19%)	12 (12%)	0.2 ³
ICU Admission	19 (8.8%)	12 (10%)	7 (7.1%)	0.4 ³

¹Median (25%-75%); n (%)
²Wilcoxon rank sum test
³Pearson's Chi-squared test

287

288 **Table S5: Characteristics and Outcomes for UAB COVID-19+ Biospecimen Cohort**
289 **Stratified by Pre-Admission Diabetic History.**

290

291 **REFERENCES**

- 292 1. Zhang J-Y et al. Single-cell landscape of immunological responses in patients with
293 COVID-19. *Nat Immunol* 2020;21(9):1107–1118.
- 294 2. Lee JS, Park S, Jeong HW, et al. Immunophenotyping of COVID-19 and influenza
295 highlights the role of type I interferons in development of severe COVID-19. *Sci Immunol.*
296 2020;5(49):eabd1554.
- 297 3. Arunachalam PS et al. Systems biological assessment of immunity to mild versus
298 severe COVID-19 infection in humans. *Science* 2020;369(6508):1210–1220.

- 299 4. Wen W et al. Immune cell profiling of COVID-19 patients in the recovery stage by
300 single-cell sequencing. *Cell Discov* 2020;6:31.
- 301 5. Tirosh I et al. Dissecting the multicellular ecosystem of metastatic melanoma by single-
302 cell RNA-seq. *Science* 2016;352(6282):189–196.